

Transport and tunneling within a compressible electron liquid in wires and rings of GaAs/Al_xGa_{1-x}As heterostructures

J. Wróbel and T. Dietl

Institute of Physics, Polish Academy of Sciences, aleja Lotników 32/46, PL-02 668 Warszawa, Poland

K. Regiński and M. Bugajski

Institute of Electron Technology, aleja Lotników 32/46, PL-02 668 Warszawa, Poland

(Received 25 February 1998)

A detailed study of low-temperature magnetoconductance in between $\nu=2$ and $\nu=3$ quantized Hall plateaus is presented. The data are obtained for disordered two-terminal submicron wires and rings defined in GaAs/Al_xGa_{1-x}As heterostructures modulation doped by Si. In the region between the plateaus, electron density of compressible liquid in the central current strip increases gradually when lowering the magnetic field. At low densities of the electrons in the strip, a sequence of peaks is detected in the dependence of conductance on the magnetic field. This unexpected effect is interpreted in terms of the Coulomb blockade associated with the charging of the current strip. In the same range of the magnetic fields, a temperature dependence of conductance, together with the absence of the Aharonov-Bohm oscillations for transport along the central strip in the ring, are taken as the evidence for an enhancement of the electron-phonon scattering rate at the percolation threshold. The frequency doubling of the Aharonov-Bohm oscillations in a ring with an additional potential barrier is discussed in terms of the phase concept. Slow time evolution of conductance is observed for higher concentrations of the electrons in the current strip. This surprising noise is attributed to glassy dynamics of localized electrons in the wire center, and to the corresponding time dependence of the impurity-assisted tunneling probability between the current carrying regions. [S0163-1829(98)03548-6]

I. INTRODUCTION

Soon after the discoveries of the integer quantum Hall effect in a two-dimensional (2D) electron gas and the conductance quantization of a one-dimensional (1D) quantum point contact, it was realized that these remarkable effects are essentially a single-electron phenomena. In particular, transport properties of 2D and 1D systems in the high magnetic fields were successfully described in terms of the skipping-orbit/edge current concept.^{1,2} The idea of a current-carrying edge state with almost zero width proved to be very useful, and made it possible to describe a vast amount of complex data obtained for mesoscopic devices in the so-called adiabatic transport regime.³

In the last decade, however, the role of many-electron effects has become more and more appreciated. Particularly, the total electrostatic energy and nonlinear screening have turned out to play an important role in the carrier redistribution in the vicinity of edges and impurity potentials.⁴ The concept of the edge currents with nonzero width was initially applied to the fractional quantum Hall effect,⁵ and then extended to the integer case.⁶ Self-consistent calculations of the many-electron energy were presented in a large number of papers⁷⁻¹³ and, gradually, their results have begun to be employed for the interpretation of experimental data. Most of the experimental studies have been devoted to edge transport either in large 2D systems¹⁴⁻¹⁷ or in quantum point contacts and zero-dimensional (0D) quantum dots.¹⁸⁻²⁰ Less attention has been given to the quantum wires, for which the theoretical models should apply most directly.

The total electrostatic energy and electron distribution in an infinite quantum wire was calculated by Chklovskii,

Matveev, and Shklovskii (CMS) (Ref. 9) adopting the Thomas-Fermi approximation. By minimizing the total energy of the wire those authors showed that edge current "strips," containing the compressible electron liquid, are formed in the high magnetic fields. Such strips are characterized by the position dependent filling factor ν , and behave like a metal — they can effectively screen external potentials. The strips are separated by insulatorlike incompressible liquid regions. More recently, this model was extended by taking into account Hartree^{21,22} and Hartree-Fock interactions.²³ Generally, more rigorous methods give results which are comparable with the CMS model, especially in the limit of the high magnetic fields and low temperatures.

In addition, CMS argued that the two-terminal conductance of an ideal wire is given by

$$G = (e^2/h) \nu_B(0),$$

where $\nu_B(0)$ is the electron filling factor in the center of the wire. Hence, if the middle strip in the channel is *incompressible*, the conductance G becomes quantized.

In our previous study^{24,25} we examined the magnetic-field-induced conductance quantization in a two-terminal ballistic wire of length $L = 1.6 \mu\text{m}$, fabricated from a high mobility ($\sim 10^6 \text{ cm}^2/\text{Vs}$) modulation-doped GaAs/Al_xGa_{1-x}As heterostructure. Rather narrow quantized plateaus were observed at 1.5 K, and their positions and widths were in good quantitative agreement with the CMS theory. The width of the plateaus was small because the current strips in the center of the channel are *compressible* in a wide range of the magnetic fields. In such a case, $\nu_B(0)$ is noninteger, and G is not quantized.

Another manifestation of the many-body interactions is the position dependent spin splitting at the edges of the 2D electron gas.^{8,26} The magnitude of spin splitting in the case of quantum wires has been considered theoretically,^{27–29} and also experimentally in our earlier work.³⁰ In particular, it has been predicted²⁷ that the electron g factor is *not* enhanced over its one-electron value (in contrast to the 2D case), provided that the kinetic energy of the edge-skipping electrons is large compared to the exchange energy. Recently, a self-consistent treatment of exchange and correlations in quantum wires has been presented.³¹ The results concerning the lack of the enhancement of the spin splitting were found³¹ to be in very good agreement with our experimental findings.³⁰

In the present paper we examine the two-terminal conductance G between quantized plateaus for more *disordered* devices. When G is not quantized the middle strip of a low-mobility channel is a mixture of incompressible (“insulator”) and compressible (“metal”) components. Furthermore, the compressible liquid in the channel center should break up into localized and delocalized regions, which form a percolation network.³² Our purpose is to determine the properties of such an intermediate state by studying the tunneling and phase coherence of electrons below and above the quantization threshold.

Samples, in the form of wires and rings were fabricated by means of electron-beam lithography of a modulation-doped GaAs/Al_xGa_{1-x}As:Si heterostructure. Additionally, one wire and one ring contained a transverse potential barrier, also patterned lithographically. The measurements were carried out down to 30 mK in the magnetic fields B up to 90 kG.

Obviously, in order to study transport properties of a disordered compressible liquid, the device length L has to be greater than the mean free path ℓ . At the same time, however, L should not be too large since in the long wires the conductance is strongly affected by backscattering *across* the sample between the two current strips. Localized states originating from the upper Landau level serve as intermediate states for such a process. As a result, the conductance on the low-field side of the plateaus is reduced below the corresponding quantized value. Such a conductance minimum (antiresonance) was theoretically predicted^{11,33–35} and observed experimentally^{30,36} in two-terminal wires. In the backscattering process, the impurity assisted acoustic-phonon scattering is presumably involved.³⁷ The efficiency of such an electron-phonon interaction in quantum wires is interesting of its own. In particular, it has been suggested that the corresponding scattering rate drops to zero when the electron drift velocity within the 1D subband becomes smaller than the sound velocity.³⁸ A detailed temperature study of the conductance antiresonances observed for a 20- μm quantum wire in the quantized magnetic field has been reported in our previous work,³⁹ and shown to corroborate the above theoretical prediction.

The organization of the present paper is following. In Sec. II, experimental details and sample characterization are described. Experimental data concerning electron transport within the compressible electron liquid for the filling factor $2 \leq \nu \leq 3$ in *quasiballistic* wires $L \geq \ell$ are discussed in Sec. III. The results suggest that Coulomb blockade effects are important for charge transport through a just-formed perco-

lation path — a sequence of conductance peaks, corresponding to a single-electron addition spectrum is observed *on* the quantized plateaus. A temperature dependence of conductance indicates, however, that inelastic processes affect also charge transport near the percolation threshold. This is supported by experimental results for the ring samples presented in Sec. IV. Electron transmission along the central current strip is by no means coherent since the Aharonov-Bohm (AB) oscillations with the fundamental frequency, clearly visible near $B=0$, are *not* observed for the ring-shaped devices in the percolation regime. We interpret these findings according to a recent theoretical model,⁴⁰ which suggests that in contrast to the vanishingly small electron-phonon scattering rate near the bottom of 1D magnetoelectric subbands in ideal wires,³⁸ the electrons at the percolation threshold are strongly coupled to the acoustic phonons.⁴⁰ At the same time, the ring containing the barrier shows frequency doubling of the AB oscillations in the plateau region, $\nu=2$. These results appear to demonstrate the validity of the phase rigidity concept^{41,42} in disordered two-terminal nanostructures under quantized magnetic fields. Section V contains results obtained for the high-magnetic-field onset of $\nu=3$ plateau (i.e., for high-density compressible liquid, far above the percolation threshold), which reveals that, surprisingly, the conductance is time dependent. It is suggested that this noise is brought about by glassy dynamics of localized electrons in the wire center, and by the corresponding time dependence of the impurity-assisted tunneling probability between the current carrying regions.

In summary, the low-temperature properties of a disordered compressible liquid can be outlined as follows (see also Sec. VI): (i) the magnetic field induced changes of the total number of percolating electrons lead to the Coulomb blockade peaks, observed on the low field side of the conductance plateaus. The period of the single-electron addition spectra is in agreement with the calculations based on the CMS model; (ii) transport within a percolating path is not coherent, presumably because the central current strip as a whole interacts with the acoustic phonons, as predicted in Ref. 40; (iii) on the high-field side of the conductance plateau G is time dependent for the disordered samples. Such noise, observed for the first time, is dominated by the presence of Lorentz-type fluctuators with only few characteristic frequencies.

II. EXPERIMENTAL DETAILS AND SAMPLE CHARACTERIZATION

The present study has been carried out on two-terminal wires and rings fabricated by means of electron beam lithography and wet etching from a modulation-doped GaAs/Al_xGa_{1-x}Si heterostructure. The Al content $x=0.3$ and the spacer width of 15 nm resulted in an electron concentration and mobility of $4 \times 10^{11} \text{ cm}^{-2}$ and $2.5 \times 10^5 \text{ cm}^2/\text{Vs}$, respectively. The epilayers were grown by molecular beam epitaxy and no special procedure for obtaining the high electron mobility was applied. The deep-level transient spectroscopy studies, carried out on layers grown at the same conditions, revealed the presence of residual impurities in the conducting channel, most probably related to Te, Se, or S.⁴³ The wires had length $L=2.1 \mu\text{m}$ (comparable to the mean

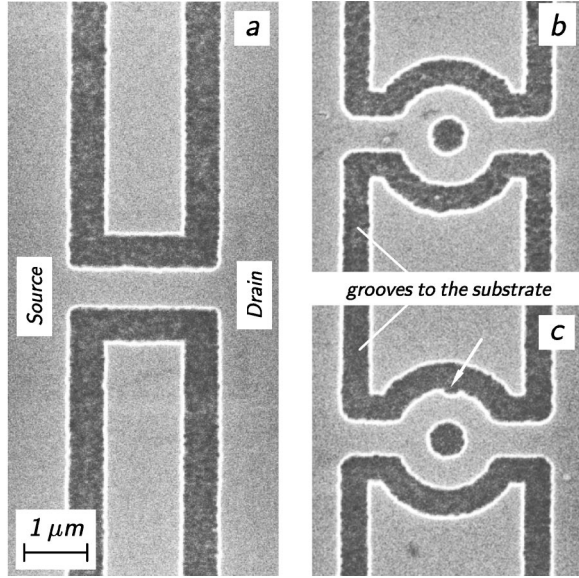


FIG. 1. Scanning electron microscope images of wet etched two-terminal quantum devices: (a) wire (b) ring, and (c) asymmetric ring with an artificial defect — a narrowing located in the upper semicircular arm (pointed out with an arrow). All pictures were taken with the same magnification — the scale is indicated in the lower left corner.

free path in 2D) and lithographic width $W_{lith} \approx 0.7 \mu$ [see Fig. 1(a)]. The ring-shaped structures had a total length of $3 \mu\text{m}$, and consisted of a central ring with an average diameter of $1 \mu\text{m}$ with two “leads” of $1 \mu\text{m}$ [see Fig. 1(b)]. The two devices (one wire and one ring) had an additional transverse potential barrier of lithographic size $50 \times 50 \text{ nm}$, located inward at one of the mesa edges, as shown in Fig. 1(c). Standard AuGeNi Ohmic contacts were formed by annealing quite close to the devices, typically $8 \mu\text{m}$ apart.

Conductance measurements were conducted in an He-4 cryostat and He-3/He-4 dilution refrigerator by employing a standard low-frequency lock-in technique with current excitation of 1 nA . Special care was taken to avoid heating of the electron gas by external noise — the cryostat was carefully grounded and the samples were connected through a set of discrete and distributed high-frequency rejecting filters.

In submicron structures the true (physical) width of electron distribution is considerably smaller than W_{lith} . In the CMS model it is assumed that the distribution of electron density across the wire, in a zero magnetic field, is given by

$$n(x) = n_0 \sqrt{(b^2 - x^2)/(d^2 - x^2)}.$$

TABLE I. Samples parameters inferred from the low-magnetic field magnetotransport: W , physical width of the device, n_{2D} , 2D electron concentration; E_F , Fermi energy, n_L , 1D electron density; parameters estimated from the parabolic confinement model: N , number of occupied 1D subbands (at $B=0$), $\hbar\omega_0$, 1D energy level separation. W_{lith} is the lithographical width of the device, n_0 is the CMS model parameter (see text).

	W_{lith} μm	W μm	n_{2D} 10^{11} cm^{-2}	E_F meV	$\hbar\omega_0$ meV	n_L 10^6 cm^{-1}	N	n_0 10^{11} cm^{-2}
Wire	0.7	0.28	2.84	10.2	0.7	8.0	14	7.75
Ring	0.6	0.17	2.59	9.3	1.2	4.4	8	11.46

The density reaches $(b/d)n_0$ at the wire center and vanishes for $x = \pm b$. This formula was derived⁴⁴ for a split-gate device with a gate distance of $2d$. Parameter d determines the shape of the electron distribution. For $d \rightarrow b$, $n(x) \equiv n_0$ whereas for $d \gg b$ the carrier distribution forms a semicircle-like profile. There are two arguments that this model can be likewise applied to the etched devices, where the electron density is also depleted near the mesa walls and is the largest at the wire center. First, for $d \gg b$ and $x \rightarrow b$ the above formula agrees well with the density profile calculated by Gelfand and Halperin²⁶ for a mesa-etched sample. Second, the width of the mesa edge depletion studied experimentally⁴⁵ is in a reasonable agreement with calculations based on a split-gate model.⁷ For our structures, the depletion region is also much wider than the true physical width of the carrier distribution (see below). In this limit, the shape of the electron density profile across the device is less sensitive to the exact value of d . Therefore we assumed $d = W_{lith}/2$.

The physical width of the electron distribution, $W = 2b$, has to be independently determined. For this purpose we use low-field magnetotransport data. In the case of wires, a resistance maximum is observed when the cyclotron radius l_c is approximately two times greater than the wire width W . This maximum is attributed to a nonspecular component of boundary scattering. Following a previous study,⁴⁶ we adopt the formula $W = 0.55 \times l_c$, and obtain for our wires $W = 0.28 \mu\text{m}$. In the case of rings we determine $W = 2b = 0.17 \mu\text{m}$ from the period of the Aharonov-Bohm oscillations in the magnetic-field range -1 kG to $+1 \text{ kG}$, see Fig. 3. The presence of the oscillations demonstrate directly that the phase coherence length is longer than $3 \mu\text{m}$ near $B = 0$.

The last unknown quantity n_0 is treated as a fitting parameter to the CMS model (see next section). By substituting its value to the formula describing $n(x)$ and averaging over the width, a 2D electron concentration n_{2D} can be calculated. The resulting value is in a good agreement with that determined from the period of the Shubnikov–de Haas oscillations in the magnetic field range $l_c \ll W$. Knowing W and n_{2D} as well as assuming the parabolic confinement we are in position to estimate 1D electron density n_L , the number of the occupied 1D levels N , and the interlevel energy distance $\hbar\omega_0$. The results are summarized in Table I. Note that for both types of the devices we obtain almost the same width of the depletion region ($\approx 0.2 \mu\text{m}$), which is of a typical magnitude for the wet etched GaAs/Al_xGa_{1-x}As devices. Note also that since W is significantly smaller than W_{lith} , the estimations based on the parabolic confinement model should lead to reasonable results. Moreover, a slowly varying para-

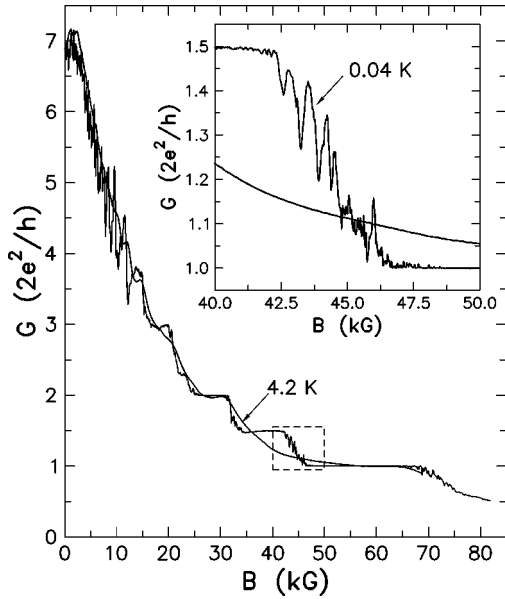


FIG. 2. The wire conductance as a function of the magnetic field at two temperatures, 0.04 K and 4.2 K. The dashed box in the main figure circumscribes the data region between $\nu=3$ and $\nu=2$ plateaus, which is shown in more detail in the inset.

bolic potential favors the formation of wider edge current strips than those expected in the case of the rectangular potential well.⁹

In Figs. 2 and 3 the two-terminal conductance G versus the magnetic field B is presented for the wire and ring, respectively. Always a small ($\sim 20 \Omega$) resistance was subtracted from the measured values, since the same pair of contacts was used as a current and voltage terminals. The additional voltage drop developed presumably on the outer parts of alloyed contacts and also on the conducting epoxy

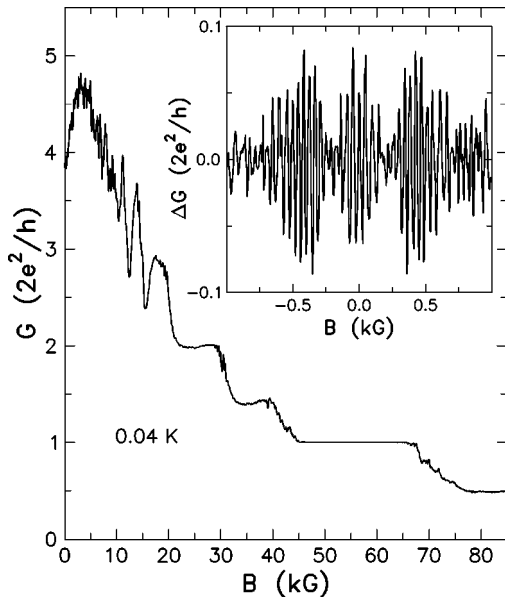


FIG. 3. The conductance for the symmetric ring measured at 0.04 K as a function of the magnetic field. The inset shows the oscillating part of the magnetoconductance, recorded around zero magnetic field (the corresponding Fourier spectrum is shown in Fig. 7).

used for bonding the current and voltage leads to the same metal pad of two-terminal wire. Note that for both devices the magnitude of the conductance in $B=0$ is about one half of the corresponding Landauer-Büttiker conductance $(2e^2/h)N$, where N is the number of 1D subbands, displayed in Table I. In the range of low magnetic fields, weak localization minima followed by universal conductance fluctuations (UCF's) are visible. These findings point to the presence of relatively large disorder, partly originating from the S impurities and partly from the mesa wall roughness, as discussed above. A magnetic field suppresses backscattering and thus reduces the role of imperfections—in the high-field range, well developed and exactly quantized conductance plateaus are seen. But *in between* the plateaus, a rich fluctuation pattern is preserved. Such fluctuations are not observed in the ballistic devices,⁴⁷ and are again connected with disorder.

Nevertheless, results presented in Fig. 2 differ in one important respect from typical data for the long and disordered wires. Namely, the conductance ‘‘antiresonances’’ are not observed. As shown in Fig. 2, there is no evidence for the presence of the antiresonances in the vicinity of either $G=1$ ($\nu=2$) or $G=2$ ($\nu=4$) plateaus. We conclude that our structures are in the quasiballistic regime, $\ell \lesssim L$.

However, near those plateaus that correspond to the spin splitting, weak antiresonances are seen. In addition, the plateaus with odd-filling factors are not as exactly quantized as the ones corresponding to the even values of ν . The latter is particularly evident for the ring structure. These observations indicate that backscattering across the sample, which involves localized states of the higher spin subband is rather effective. This points, in turn, to the existence of spin non-conserving processes as well as to a small magnitude of the spin splitting. The latter is corroborated by a quick disappearance of the plateaus corresponding to the odd ν values with the increasing temperature. Indeed, Eqs. (12) and (13) from Ref. 27 predict a small magnitude of the spin splitting up to 180 kG and 150 kG for our wire and ring, respectively. To emphasize a minor importance of the spin splitting in the studied structures we present the conductance in the $2e^2/h$ units.

III. TRANSPORT WITHIN A COMPRESSIBLE STRIP

Figure 4 shows an expanded view of $G=1$ ($\nu=2$) plateau, as measured for the wire-shaped structure at low- and high-temperature limits. The values of $(e^2/h)\nu(0)$ versus magnetic field, calculated according to CMS model,⁹ are also shown. In the upper part of Fig. 4, the calculated positions of the current strips are depicted.

CMS theory predicts a very narrow plateau (of the width of ~ 5 kG) since G is quantized only in the case when electron liquid in the center of the wire is incompressible. This occurs in a rather limited range of the magnetic fields. For the device under consideration, when the magnetic field is lowered, the compressible metal-like strip starts to develop in the middle of the wire already in $B \approx 61$ kG according to CMS theory. In practice, however, G remains exactly quantized in the lower fields because the compressible channel has initially a very low density so that the electrons are localized by disorder. With a further decrease of the magnetic

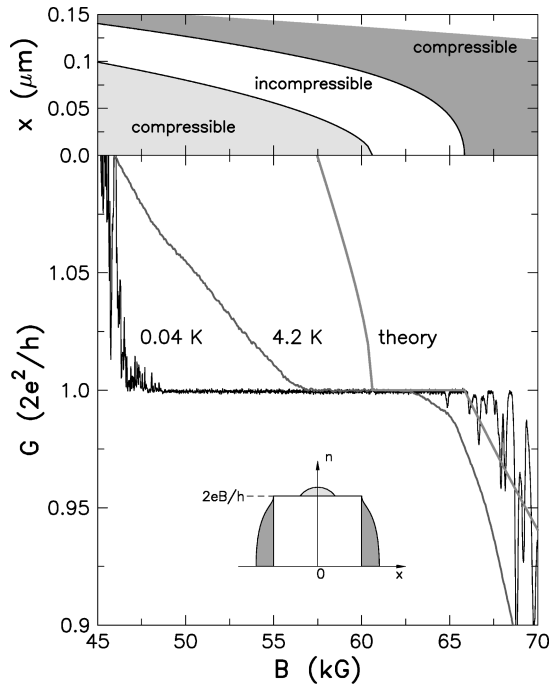


FIG. 4. The conductance in the plateau region ($G \sim 1, \nu = 2$) for the wire, presented already in Fig. 2. The width of compressible electron liquid as a function of the magnetic field, calculated within the Chklovskii, Matveev, and Shklovskii (CMS) model (Ref. 9) is shown in the upper part of the figure. The conductance of an ideal wire, $G = (e^2/h) \nu_B(0)$, is shown by the thick gray line. The electron distribution across the wire (for $B \sim 57$ kG) is depicted schematically.

field, the density of the compressible liquid increases and, eventually, the central strip starts to conduct. At $T = 4.2$ K, this happens in $B \approx 57$ kG, when the electron strip has a width of $0.085 \mu\text{m}$ and the density of the compressible liquid reaches $3.0 \times 10^{10} \text{ cm}^{-2}$ in the wire center.

As expected, the width of the plateaus increases with the lowering of temperature. This is mainly due to the fact that localization is more effective at low temperatures, at which the inelastic scattering length becomes longer than the localization radius. At the same time, our data are in good qualitative agreement with recent self-consistent numerical calculations of the magnetoconductance of short quantum wire ($L = 0.5, W = 0.33 \mu\text{m}$) with an additional central constriction.⁴⁸ The plateau widths calculated in that paper are larger than those expected from the CMS model. Moreover, the widening increases with decreasing temperature, and it occurs on the low-field side of the plateaus, as indeed observed experimentally in our structures.

Nevertheless, even at the lowest temperatures ($T = 0.04$ K) the conductance somewhat increases with decreasing B but in a nonmonotonic way. A sequence of sharp conductance peaks is observed on the low-field side of the plateau. This feature is entirely determined by transport within the compressible liquid as the antiresonances are absent and $G \geq 1$.

It is possible that the observed peaks result from sequential tunneling *along* the wire between closed current loops near the percolation threshold. The most efficient are processes involving resonant tunneling *via* an intermediate state

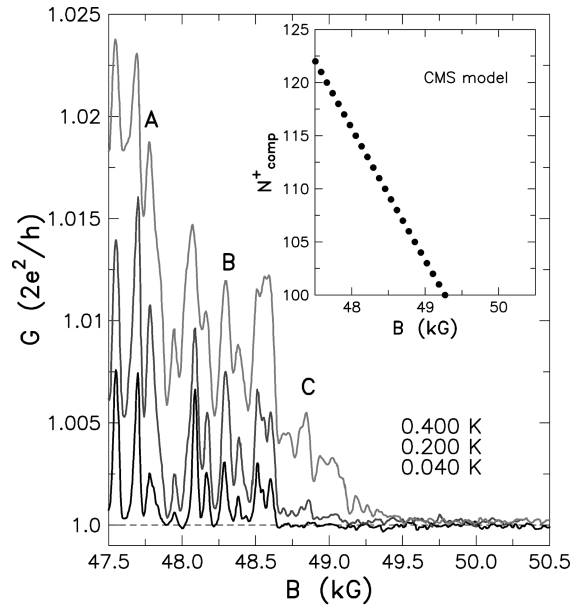


FIG. 5. Coulomb blockade peaks observed on the low-field arm of $G = 1, \nu = 2$ plateau for the wire, measured at 0.4, 0.2, and 0.04 K (top to bottom). Inset shows the estimated number of spin polarized electrons in the central compressible strip. We assumed $N_{comp}^+ \approx (1/2)N_{comp}$. The temperature dependence of conductance in the magnetic fields labeled A, B, and C is shown in the next figure.

having character of a dot with the edge current circulating around.^{3,49} If the magnetic field is changed, the zero-dimensional states of such a dot cross sequentially the Fermi energy any time the magnetic flux through its diameter is changed by one flux quantum.⁵⁰ The resulting single-electron resonant tunneling produces conductance peaks, indeed observed experimentally in quantum wires in high magnetic fields.^{51,52} In our sample this corresponds to the field range between 42 kG and 45 kG in Fig. 2.

However, resonant tunneling alone cannot account for a large number of the conductance peaks superimposed on the $\nu = 2$ plateau, for $B > 45$ kG. The peaks, shown in more details in Fig. 5, are quasiperiodic in B with an average period equal approximately to 110 Gs. This value would correspond to an average “dot” diameter of $0.7 \mu\text{m}$, which appears to be quite unrealistic. We attribute the conductance maxima shown in Fig. 5 to the field-induced change in the number of the “compressible” electrons one by one. In other words, we assume that a charging energy related to the single electron transfer through the wire modulates the conductance of the just-formed percolation path — similarly to the case of the Coulomb blockade for tunneling through a quantum dot.⁵³ Such an effect is absent in both ballistic $L \ll \ell$ and long $L \gg \ell$ wires since in the former case a large transmission coefficient $T = 1$ reduces the probability of a simultaneous presence of several electrons in the wire while in the long conductors the charging energy is small.

Since its discovery by Scott-Thomas,⁵⁴ the phenomenon of the Coulomb blockade in semiconductor nanostructures has attracted a considerable attention (for recent review see⁵⁵). In the case of disordered wires in magnetic field, the charging effects were studied by Staring *et al.*⁵⁶ for devices defined by a split gate on a GaAs/Al_xGa_{1-x}As heterostructure. Those authors reported on the observation of periodic

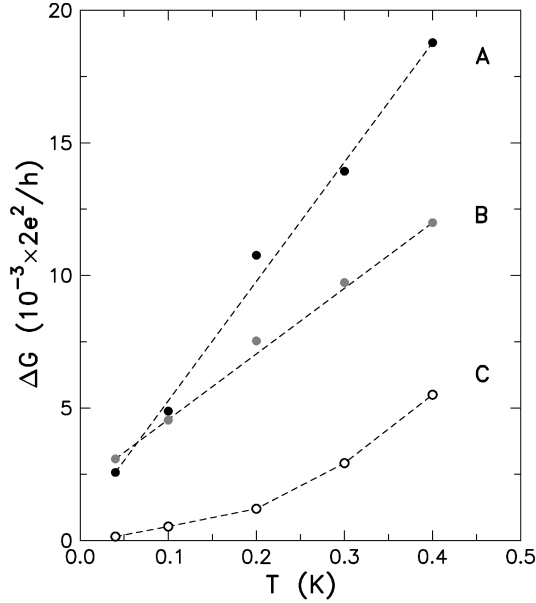


FIG. 6. The amplitude of the three selected conductance maxima (see previous figure) as a function of temperature.

conductance oscillations as a function of the gate voltage, observed close to the pinch-off, and attributed them to tunneling modified by the effect of the Coulomb blockade.

In the self-consistent picture, the peaks observed by us may correspond to the population of the central strip—treated as a whole—by a single electron. In the CMS model the number of “compressible” electrons “floating” on top of the incompressible liquid (with $\nu=2$, which acts as a sort of a reservoir) is given by

$$\Delta n_{comp} = n_L(\nu_B(0) - 2)$$

in the center of the wire, where $n_L = eB/h$. Since the width of the central current strip is known (see Fig. 4), the total number of spin-polarized compressible electrons can be evaluated as a function of B . The results are shown in the inset to Fig. 5. According to such a calculation, the number of the compressible electrons changes by twelve per kG between 47 and 50 kG, which is in remarkable agreement with the experimental period of 110 Gs.

When the temperature is raised, the width and height of the conductance peaks increase monotonically but their positions remain unchanged, as shown in Fig. 5. A similar behavior was reported⁵⁶ for the gate-induced Coulomb-blockade oscillations. Furthermore, when the sample is heated, more peaks of the electron addition spectrum appear on the high-field side of the plateau. In the spirit of the CMS model, this can be explained as an increase in the number of delocalized electrons with temperature. It is also possible that the percolation path is more strongly coupled to the leads when T is raised.⁵⁷ The self-capacitance C and charging energy $e^2/2C$ of the central compressible strip can be estimated from its size. On the low-field side of the plateau $e^2/2C \approx 0.2$ meV. This value is consistent with the disappearance of the peaks at $T \geq 2$ K.

Figure 6 shows the conductance of compressible liquid, $\Delta G = G - 1$, as a function of temperature for three characteristic values of the magnetic field (denoted A , B , C in the

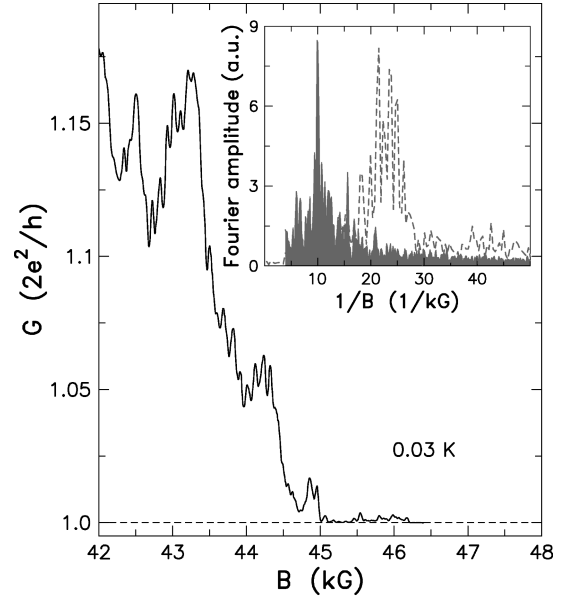


FIG. 7. The low-magnetic field side of the $G=1, \nu=2$ plateau obtained for the ring at 0.03 K. The inset shows the Fourier spectrum of the oscillating part of the conductance. For comparison, the Fourier amplitude of weak-field ($|B| < 1$ kG) Aharonov-Bohm oscillations is also shown (dashed line).

previous figure). ΔG is seen to increase monotonically with T . Recently, it was shown that the percolation path can globally emit or absorb acoustic phonons in strong magnetic fields, with the rate proportional to T , if only the drift velocity is very small, i.e., just on the percolation threshold.⁴⁰ We believe that this assumption corresponds to the experimental conditions under consideration. It appears, therefore, that the electron-phonon interaction is the dominant inelastic process leading to apparent delocalization of compressible liquid, and thus to the increase with temperature of its conductivity. As discussed in the next section, this interaction constitutes also an efficient phase breaking mechanism.

IV. AHARONOV-BOHM EFFECT IN QUANTIZED MAGNETIC FIELDS

It is natural to ask whether it would be possible to observe the Aharonov-Bohm (AB) oscillations in a ring-shaped structure in the quantizing magnetic fields. When the current flows through a percolation path in the channel center one could expect the AB oscillations to have the same frequency f_0 as those near $B=0$ presented in Fig. 3. Figure 7 shows the ring conductance on the low- B side of the plateau that corresponds to $G=1$ ($\nu=2$). The oscillations, with the amplitude greater than that assigned to the Coulomb blockade, are visible. In the inset to Fig. 7 the Fourier spectrum is depicted; it was computed after filtering out slowly varying background conductance. The oscillations are periodic but their frequency f_B is approximately equal to $(1/2)f_0$.

An unexpected doubling of the AB period was recently reported by Bird and co-workers^{58,59} for a quantum dot coupled to large 2D regions. In our case, however, the period doubling appears to be purely accidental. As suggested by Timp *et al.*⁶⁰ and sketched in Fig. 8a, the observed AB oscillations are very likely associated with resonant tunneling

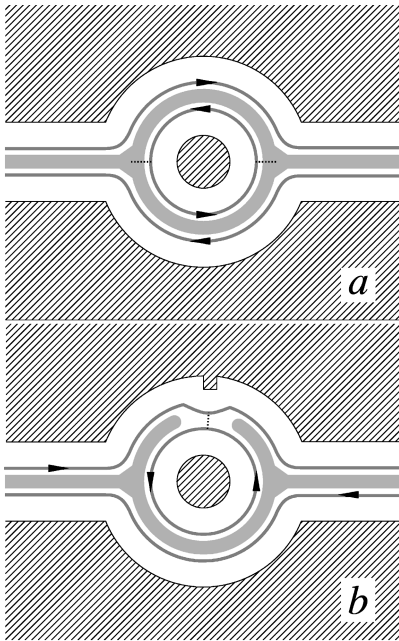


FIG. 8. A schematic representation of two possible tunnelling processes, responsible for the high magnetic field Aharonov-Bohm oscillations with the frequency f_B and $2f_B$. Light gray areas represent low-density compressible liquid, darker lines correspond to the high-density edge currents. The arrows indicate the direction of current flow. (a) Tunnelling at the entrance and at the exit to the ring. (b) Additional tunnelling that occurs at the vicinity of an artificial narrowing.

between the central strips in the two current leads *via* those edge states that correspond to $\nu=2$ and circulate around the inner hole. The transition probability through such a dotlike state is known^{49,3,50} to undergo the AB oscillations. The spatial position of these circulating states evaluated within the CMS model agrees very well with that deduced from the measured AB frequency f_B .

From the data presented here we conclude also that electron transport through the central strip is *not* coherent as the AB effect of the frequency f_0 is not observed. This means that the inelastic mean free path is particularly short for this strip as the coherence is maintained for electron transport through the inner shell as well as near $B=0$. Following theoretical considerations⁴⁰ we note that particularly efficient electron-phonon scattering is expected at the percolation threshold, where a complex spatial form of the carrier wave functions allows for the coupling to phonons from a wide range of the wave vectors. The latter shows why the inelastic-scattering length is the shortest for the central current strip, and explains a decrease of the AB frequency with the magnetic field, an effect already reported by Timp *et al.*⁶⁰ for multiterminal devices.

A further insight into tunneling processes can be gained from data collected for a similar ring but having an artificial narrowing in one of the semicircular arms. Figure 9 shows the low-temperature $G(B)$ data obtained for such a structure. As expected, the conductance at $B=0$ is smaller as compared to the “ideal” ring, and the exactly quantized $G=1$ plateau is observed in weaker fields. On the low-field arm of the plateau (from 30 to 35 kG), strong conductance oscillations with the frequency f_B are observed, as before.

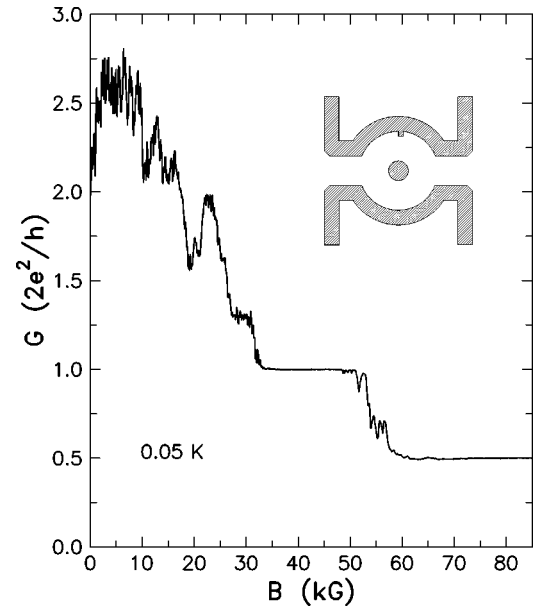


FIG. 9. The conductance for asymmetric ring (with an artificial narrowing), at 0.05 K.

However, a different behavior is detected when G values are very close to 1. Figure 10 shows the conductance (for $35 < B < 42$ kG) and the Fourier spectrum of its oscillating component. In contrast to the data for the ideal ring, weak oscillations of a nonmonotonic amplitude and the frequency f_B are observed *on the quantized plateau* (see also Fig. 11). The “on-plateau” oscillations are seen to lower an average magnitude of G below its quantized value, $G=1$. This implies that the effect is produced by backscattering. A straightforward interpretation of this observation is that the constriction provides an additional channel for tunneling between the compressible liquids, which is efficient even in the field

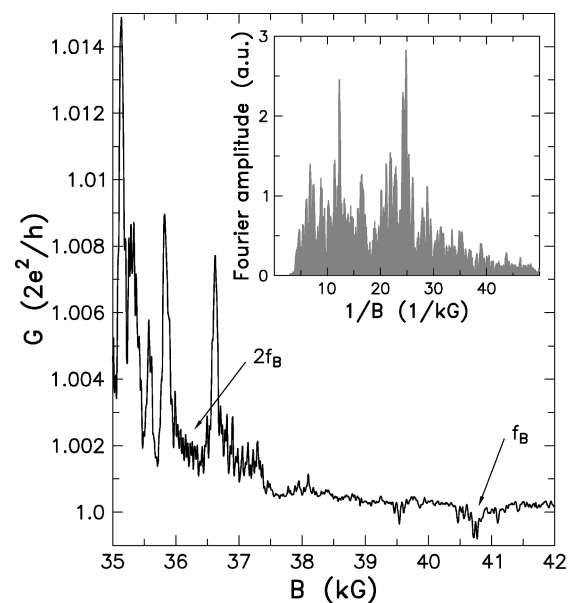


FIG. 10. The low-field side of conductance plateau $G=1, \nu=2$ measured for the asymmetric ring (with an artificial narrowing) at 0.03 K. Fourier spectrum of the oscillating part of the conductance is shown in the inset.

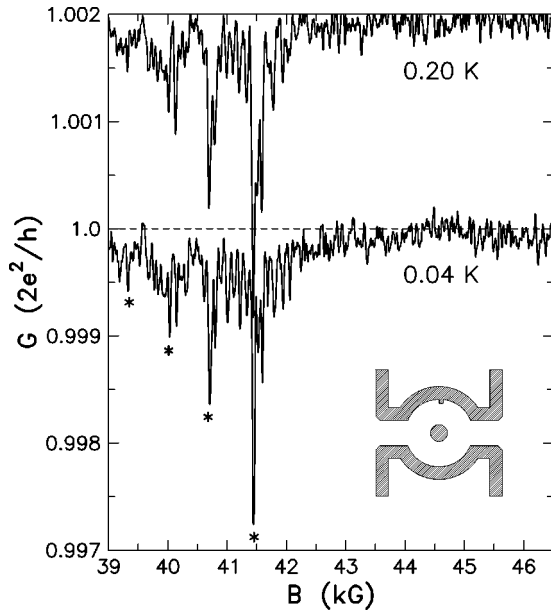


FIG. 11. A highly enlarged view of conductance plateau $G=1, \nu=2$, obtained for asymmetric ring (with an artificial narrowing). Data for $T=0.2$ K are shifted upward for clarity. Note the presence of narrow peaks (marked with stars), which we attribute to the Coulomb blockade of charging of the inner current strip.

range, for which no tunneling occurs in the ideal ring. Now, since the electrons in one of the involved strips circulate around the ring, the tunneling probability is modulated by the corresponding Aharonov-Bohm frequency.

As already mentioned, the amplitude of the oscillations corresponding to on-plateau backscattering is highly non-monotonic, and is also found to decrease with temperature. Strong additional conductance minima, marked with a star symbol in Fig. 11, are attributed to single-electron charging of the inner edge state. The observed Aharonov-Bohm effect is, therefore, superimposed on the Coulomb-blockade peaks but, in contrast to the situation discussed in Sec. III, the electrons are removed or added to the central circulating strip, *not* to the just-formed percolation path.

Moreover, again in contrast to the symmetric device, weak oscillations with double frequency $\sim 2f_B$ are found in somewhat lower fields, just at the onset of conductance quantization. Frequency doubling has been noted in several studies of the AB effect in dots and antidots.^{61–64} It has been interpreted as originating from spin-resolved oscillations, locked in the anti-phase. It is not clear, however, how a superposition of two independent periodic signals could lead to the frequency doubling. More probably, in two-terminal Aharonov-Bohm devices, the frequency doubling may occur as a result of a constrain imposed by the Onsager-Büttiker symmetry relations,⁶⁵ $G(B) = G(-B)$. Experimentally, such an effect was demonstrated by inserting a potential barrier for the electrons in a two-terminal AB ring.^{41,42} In particular, Yacoby, Schuster, and Heiblum⁴¹ examined the evolution of low-field AB interference as a function of the barrier height, controlled by a gate voltage. They found that indeed the phase of the h/e oscillations assumes only the two values that are allowed by symmetry: 0 and π . At the same time, for the range of the gate voltage corresponding to the transition region between the above two cases, only a weak $h/2e$

harmonic of the oscillations was detectable, i.e., the frequency doubling was observed. Of course, the effect of the phase rigidity should be preserved in the quantized magnetic fields. In the case of our sample, the magnetic field—by controlling the population of the strips—might play a role of the gate voltage. In more microscopic terms, the presence of $2f_B$ harmonic in the oscillation spectrum means that either processes involving double encircling of the ring remain coherent or that a sequential tunneling, described by a product of two transition probabilities, is operating.

V. THE TIME DEPENDENT CONDUCTANCE

So far we have considered the conductance in the high-field range of the transition region between $G=1.5$ and $G=1$ plateaus, where low-density compressible liquid, located in the center of the wire, was responsible for the transport properties. In this section, we look at the low-field portion of the intermediate region, where strips of compressible liquid reside on the two sides of the wire center. Consequently, a deviations from the quantized value of $G=1.5$ are caused by electron transitions between the strips. The sound velocity is greater than that of the electrons in the strips, so that phonon-assisted tunnelling is not efficient. If, however, the strips become sufficiently close, elastic scattering between the strips *via* states localized in the wire center may operate. Such a resonant tunneling is supposed to be much more efficient than either direct or two-step incoherent tunnelling between the current carrying strips. Since the relevant intermediate states have to lie within the range $k_B T$ around the Fermi level, their number increases, and thus G decreases, with the temperature. Such a temperature dependence is opposite to that observed in the higher fields, at which both thermal spread of electron energies and inelastic scattering *enhances* charge transport, as discussed in the previous Section.

Surprisingly, in the resonant tunneling region, G changes as a function of time. The normalized noise magnitude (ΔG) is rather large, reaching $0.03 \times (2e^2/h)$ at the lowest temperatures and for the time constant of the lock-in amplifier set at 0.1 s. The range of the filling factors, where the time dependence occurs, corresponds to $3 \leq \nu_B(0) \leq 2.4$ (compare again data presented in Fig. 2). A similar magnitude of noise was observed for all wire samples in the above range of ν values. The appearance of noise in the optical properties of 2D electrons was reported by Kukushkin *et al.*,⁶⁶ however, for much smaller filling factors ($\nu < 0.28$). Therefore, the observed fluctuations of the luminescence signal were attributed to the depinning of the Wigner solid.

The temporal evolution of conductance is shown in Fig. 12. The data were recorded at various temperatures but in the same magnetic field $B=44.2$ kG. For a comparison, time series obtained on-plateau, i.e., for $B=48.4$ kG and $G \cong 1$, is presented in the upper part of Fig. 12. In the scale of Fig. 12, the latter shows time dependence determined by the instrumental noise, as expected for the region, in which G is quantized. This result demonstrates also that the amplitude of any background noise is far below the temporal changes found in the fields corresponding to tunneling between the strips.

Conductance noise reveals few characteristic frequencies,

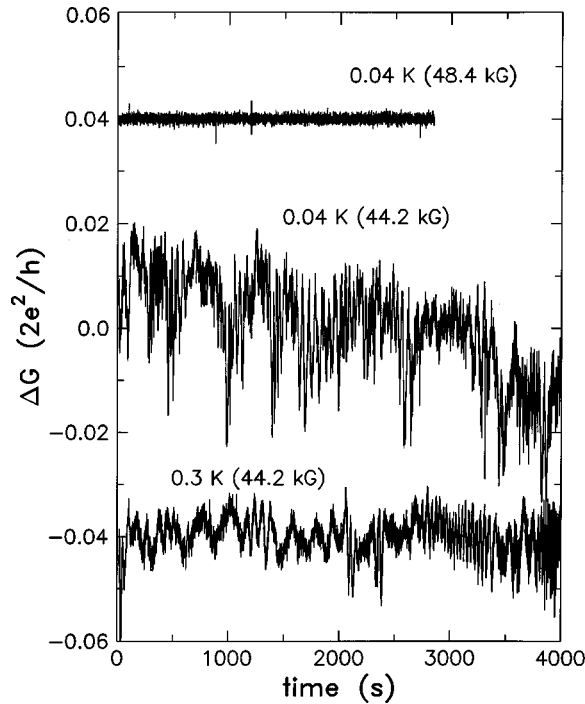


FIG. 12. Conductance variations, $\Delta G = G - \langle G \rangle$ as a function of time, recorded for the wire in the plateau region (uppermost trace), and in the region corresponding to $2.5 < \nu < 3$; $\langle G \rangle$ is the time average conductance; temperatures and magnetic fields are indicated, the latter in parenthesis. Data for 0.04 K (48.4 kG) are shifted upward and data for 0.3 K (44.2 kG) are shifted downward for clarity. Conductance was measured with a lock-in amplifier time constant of 0.1 s.

which dominate, during a finite period, the temporal evolution. With the increasing temperature the magnitude of noise decreases and the characteristic frequencies become larger. This is illustrated in Fig. 13, where Fourier power spectra of conductance noise $S(f)$ are presented. As shown, over a limited range of frequencies, $P(f) = A(T)/f^{\gamma(T)}$, where both $A(T)$ and $\gamma(T)$ decrease with the temperature. The observed value of $\gamma = 2.0 \pm 0.2$ at the lowest temperature suggests that a sum of high frequency tails of Lorentzian distributions is observed. This would mean that the noise is driven by an ensemble of fluctuators with switching times longer than 1000 s at 50 mK. When the temperature increases, the switching frequencies are expected to increase also, which explains a gradual transition towards a canonical $1/f$ noise. At the same time, more and more parallel tunnelling paths become available for the electrons, which leads to decrease of both G and the amplitude of its temporal variations, $A(f)$.

A question arises as to what the dominant mechanism that accounts for the observed noise is. First of all, we note that its large magnitude indirectly confirms the importance of resonant tunneling, which should be particularly sensitive to the actual potential landscape and to the occupancy of intermediate states. Secondly, the single-electron shot noise, as a phenomenon with a flat power spectrum, can be excluded. From a comprehensive study of noise in quantum point contacts, Liefrink, Dikhuis, and van Houten⁶⁷ concluded that G changes as a result of trapping and detrapping of electrons in the vicinity of the constriction. By changing the charge state, an electron trap shifts the potential energy of the device, and

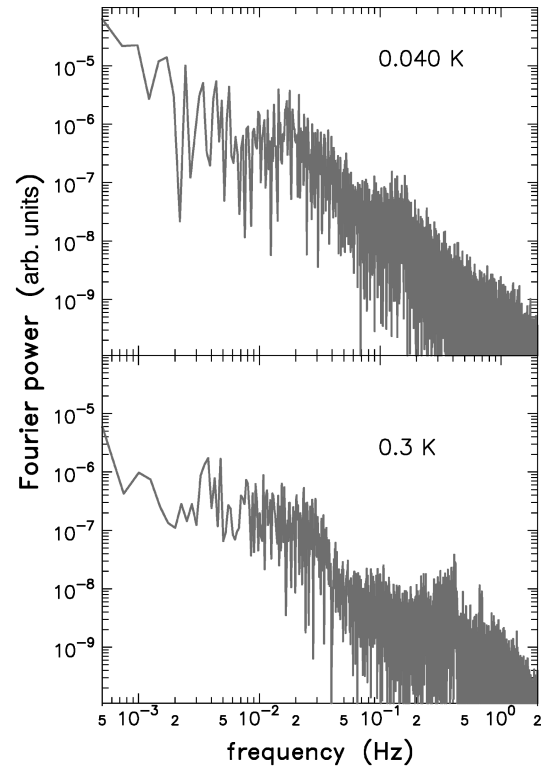


FIG. 13. The Fourier power spectra of conductance time series (ΔG data of Fig. 12) obtained over a 4000-s time interval.

thus produces a conductance jump. While such a mechanism may also operate in our case, an effect associated with slow glassylike dynamics of the hopping between localized states in the wire center could also be involved. The dynamic screening of a slowly varying potential landscape should be as well considered, especially at low temperatures.

VI. CONCLUSIONS

Our work has demonstrated that a study of low-temperature two-terminal conductance for disordered but relatively short ($L \gtrsim \ell$) wires and rings provides a worthwhile opportunity to probe the dominant mechanisms which underline electron transport in the regime of low- and high-density compressible current strips, produced by the quantizing magnetic fields. At low densities of the electrons in the strip, a sequence of peaks has been observed in the dependence of the conductance on the magnetic field. A quantitative analysis, particularly evaluation of the distance between the peaks, has lead us to conclude that the effect reflects the Coulomb blockade, associated with the charging of the current strip. In the same range of the magnetic fields, by examining both the temperature dependence of conductance and the period of the Aharonov-Bohm oscillations for transport along the central strip in the ring, we have put into the evidence the presence of enhancement of the electron-phonon scattering rate at the percolation threshold. We have also suggested that the frequency doubling of the Aharonov-Bohm oscillations in a ring with an additional potential barrier provides a support for the concept of the phase rigidity.

Finally, our findings have revealed the time dependence of the conductance in the regime of the high concentrations of the electrons in the current strip. We have assigned this surprising noise to glassy dynamics of localized electrons in the wire center, and to the corresponding time dependence of the impurity-assisted tunneling probability between the current curing strips.

ACKNOWLEDGMENTS

The authors thank M. Guziewicz, E. Kamińska, and E. Papis for the assistance in making Ohmic contacts. One of us (J.W.) acknowledges the kind help of B. Chklovskii in clarifying some aspects of the CMS model. This work was supported by Polish KBN Grants No. PB 2-P03B-6411 and PBZ No. 28.11/P9.

- ¹B. I. Halperin, *Phys. Rev. B* **25**, 2185 (1982).
- ²J. Kucera and P. Streda, *J. Phys. C* **21**, 4357 (1988).
- ³C. W. J. Beenakker and H. van Houten, in *Solid State Physics*, edited by H. Ehrenreich and D. Turnbull (Academic, New York, 1991), Vol. 44, Chap. 1.
- ⁴A. L. Efros, *Solid State Commun.* **67**, 1019 (1988).
- ⁵C. W. J. Beenakker, *Phys. Rev. Lett.* **64**, 216 (1990).
- ⁶A. M. Chang, *Solid State Commun.* **74**, 871 (1990).
- ⁷D. B. Chklovskii, B. I. Shklovskii, and L. I. Glazman, *Phys. Rev. B* **46**, 4026 (1992).
- ⁸J. Dempsey, B. Y. Gelfand, and B. I. Halperin, *Phys. Rev. Lett.* **70**, 3639 (1993).
- ⁹D. B. Chklovskii, K. A. Matveev, and B. I. Shklovskii, *Phys. Rev. B* **47**, 12 605 (1993).
- ¹⁰N. R. Cooper and J. T. Chalker, *Phys. Rev. B* **48**, 4530 (1993).
- ¹¹M. M. Fogler and B. I. Shklovskii, *Phys. Rev. B* **50**, 1656 (1994).
- ¹²M. M. Fogler, E. I. Levin, and B. I. Shklovskii, *Phys. Rev. B* **49**, 13 767 (1994).
- ¹³I. A. Larkin and J. H. Davies, *Phys. Rev. B* **52**, 5535 (1995).
- ¹⁴N. B. Zhitenev, R. J. Haug, K. V. Kiltzing, and K. Eberl, *Phys. Rev. Lett.* **71**, 2292 (1993).
- ¹⁵S. W. Hwang, D. C. Tsui, and M. Shayegan, *Phys. Rev. B* **48**, 8161 (1993).
- ¹⁶S. Takaoka, K. Oto, H. Kurimoto, and K. Murase, *Phys. Rev. Lett.* **72**, 3080 (1994).
- ¹⁷R. J. F. van Haren, F. A. P. Blom, and J. H. Wolter, *Phys. Rev. Lett.* **74**, 1198 (1995).
- ¹⁸C. M. Marcus, R. M. Westervelt, P. F. Hopkins, and A. C. Gosard, *Surf. Sci.* **305**, 480 (1994).
- ¹⁹J. P. Bird *et al.*, *Phys. Rev. B* **50**, 14 983 (1994).
- ²⁰D. C. Glatli and C. Pasquier, in *Mesoscopic Quantum Physics*, edited by E. Akkermans, G. Montambaux, J.-L. Pichard, and J. Zinn-Justin (Elsevier Science, Amsterdam, 1995), pp. 721–730.
- ²¹T. Suzuki and T. Ando, *Physica B* **227**, 46 (1996).
- ²²T. Ando, in *23rd International Conference on the Physics of Semiconductors*, edited by M. Scheffler and R. Zimmermann (World Scientific, Singapore, 1996), pp. 59–67.
- ²³T. H. Stoof and G. E. W. Bauer, *Phys. Rev. B* **52**, 12 143 (1995).
- ²⁴J. Wróbel *et al.* (unpublished).
- ²⁵J. Wróbel, *Acta Phys. Pol.* **90**, 691 (1996).
- ²⁶B. Y. Gelfand and B. I. Halperin, *Phys. Rev. B* **49**, 1862 (1994).
- ²⁷J. M. Kinaret and P. A. Lee, *Phys. Rev. B* **42**, 11 768 (1990).
- ²⁸L. Brey, J. J. Palacios, and C. Tejedor, *Phys. Rev. B* **47**, 13 884 (1993).
- ²⁹T. Suzuki and T. Ando, *J. Phys. Soc. Jpn.* **62**, 2986 (1993).
- ³⁰J. Wróbel *et al.*, *Surf. Sci.* **305**, 615 (1994).
- ³¹O. G. Balev and P. Vasilopoulos, *Phys. Rev. B* **56**, 6748 (1997).
- ³²D. B. Chklovskii and P. A. Lee, *Phys. Rev. B* **48**, 18 060 (1993).
- ³³J. K. Jain and S. A. Kivelson, *Phys. Rev. Lett.* **60**, 1542 (1988).
- ³⁴B. Kramer, J. Mašek, V. Špička, and B. Velický, *Surf. Sci.* **229**, 316 (1990).
- ³⁵J. M. Kinaret and P. A. Lee, *Phys. Rev. B* **43**, 3847 (1991).
- ³⁶R. G. Mani and K. v. Klitzing, *Phys. Rev. B* **46**, 9877 (1992).
- ³⁷H. L. Zhao and S. Feng, *Phys. Rev. Lett.* **70**, 4134 (1993).
- ³⁸T. Brandes and B. Kramer, *Solid State Commun.* **88**, 773 (1993).
- ³⁹J. Wróbel *et al.*, *Europhys. Lett.* **29**, 481 (1995).
- ⁴⁰S. Iordanski and Y. Levinson, *Phys. Rev. B* **53**, 7308 (1996).
- ⁴¹A. Yacoby, R. Schuster, and M. Heiblum, *Phys. Rev. B* **53**, 9583 (1996).
- ⁴²G. Cernicchiaro *et al.*, *Phys. Rev. Lett.* **79**, 273 (1997).
- ⁴³M. Kaniewska *et al.*, *Acta Phys. Pol. A* **88**, 775 (1995).
- ⁴⁴I. A. Larkin and V. B. Shikin, *Phys. Lett. A* **151**, 335 (1990).
- ⁴⁵K. K. Choi, D. C. Tsui, and K. Alavi, *Appl. Phys. Lett.* **50**, 110 (1987).
- ⁴⁶T. J. Thornton, M. L. Roukes, A. Scherer, and B. P. van de Gaag, *Phys. Rev. Lett.* **63**, 2128 (1989).
- ⁴⁷B. J. van Wees *et al.*, *Phys. Rev. B* **43**, 12 431 (1991).
- ⁴⁸M. Stopa *et al.*, in *Quantum Coherence and Decoherence*, edited by K. Fujikawa and Y. A. Ono (Elsevier Science, Amsterdam, 1996), p. 211.
- ⁴⁹J. A. Simmons *et al.*, *Phys. Rev. B* **44**, 12 933 (1991).
- ⁵⁰U. Sivan and Y. Imry, *Phys. Rev. Lett.* **61**, 1001 (1988).
- ⁵¹J. A. Simmons *et al.*, *Phys. Rev. Lett.* **63**, 1731 (1989).
- ⁵²A. K. Geim *et al.*, *Surf. Sci.* **305**, 624 (1994).
- ⁵³P. McEuen *et al.*, *Phys. Rev. Lett.* **66**, 1926 (1991).
- ⁵⁴J. H. F. Scott-Thomas *et al.*, *Phys. Rev. Lett.* **62**, 583 (1989).
- ⁵⁵U. Meirav and E. B. Foxman, *Semicond. Sci. Technol.* **10**, 255 (1995).
- ⁵⁶A. A. M. Staring, H. van Houten, C. W. J. Beenakker, and C. T. Foxon, *Phys. Rev. B* **45**, 9222 (1992).
- ⁵⁷Y. Meir, N. S. Wingreen, and P. A. Lee, *Phys. Rev. Lett.* **66**, 3048 (1991).
- ⁵⁸J.P. Bird, K. Ishibashi, Y. Aoyagi, and T. Sugano, *Phys. Rev. B* **53**, 3642 (1996).
- ⁵⁹J. P. Bird *et al.*, *Superlattices Microstruct.* **22**, 57 (1997).
- ⁶⁰G. Timp *et al.*, *Phys. Rev. B* **39**, 6227 (1989).
- ⁶¹R. P. Taylor *et al.*, *Phys. Rev. Lett.* **69**, 1989 (1992).
- ⁶²A. Sachrajda *et al.*, *Phys. Rev. B* **47**, 6811 (1993).
- ⁶³A. Sachrajda *et al.*, *Phys. Rev. B* **50**, 10 856 (1994).
- ⁶⁴C. Ford *et al.*, *Phys. Rev. B* **49**, 17 456 (1994).
- ⁶⁵M. Büttiker, Y. Imry, and R. Landauer, *Phys. Lett.* **96A**, 365 (1983).
- ⁶⁶I. V. Kukushkin *et al.*, *Phys. Rev. B* **45**, 4532 (1992).
- ⁶⁷F. Liefrink, J. I. Dijkhuis, and H. van Houten, *Semicond. Sci. Technol.* **9**, 2178 (1994).